Journal of Physical Science Research and Review Volume-1, Issue:1- September 2025

VISWAM PUBLICATIONS

Journal of Physical Science Research and Review

https://viswampublications.com/journals/index.php/jpsrr



Structural, Optical, and Dielectric Properties of LCN Single Crystals

G.J. Shanmuga Sundar[a,b] N. Jesmin[c,] S. Tamilselvan[b], S. Pugazhendhi[c] and M. Vimalan[c*]

[a]Department of Physics, Rajeswari Vedachalam Government Arts College, Chengalpattu, 603 002, Tamilnadu, India.

[b]P.G & Research Department of Physics, Arignar Anna Govt. Arts College, Cheyyar, Tamilnadu 604 407, India.

[c]Department of Physics, Saveetha School of Engineering, Saveetha Institute of Medical and Technical Sciences (SIMATS), Chennai 602 105, Tamil Nadu, India.

ARTICLE INFO

Received : 19.03.2025
Revised : 17.06.2025
Accepted : 26.08.2025
Published : 15.09.2025

Corresponding author:
Dr. M. Vimalan
myresearch1121@gmail.com

Keywords:
Crystal Growth,
Optical,
Mechanical,
Dielectric,
NLO.

ABSTRACT

A new organic nonlinear optical material, L-cysteinium nitrate (LCN), has been synthesized and grown as a single crystal. It was found that the system of the crystal structure by X-ray diffraction is orthorhombic with a noncentrosymmetric space group in favour of second harmonic generation. The material has good optical transmission properties with 220 nm considered to be its cut-off in the UV area and 5.63 eV being its optical band gap. It is worth mentioning that the second harmonic generation efficiency of LCN was found to be 1.5 times the commonly used nonlinear optical crystal, potassium dihydrogen phosphate (KDP). Mechanical characterization studies have found that the material is soft in nature, showing load-dependent behavior. Dielectric studies give information about the low refractive index and extinction coefficient at a high frequency, thus showing the films to have good optical quality. Thus, with such fine properties, LCN is anticipated to be a promising candidate for integrated photonic and electro-optic devices.

This article is licensed under Creative Commons Attribution-Non-commercial 4.0 International License.
Copyright©2025 Author(s) retains the copyright of this article. DOI:

1. INTRODUCTION

In the current period, the utilisation of single crystals has made a substantial contribution to scientific developments in many domains. Nonlinear optical (NLO) materials are predicted to play an important role in photonics technology, particularly optical data processing. The discovery and development of extremely efficient NLO crystals in the visible and ultraviolet (UV) ranges is critical for developing laser processing. As a result, there is a considerable interest in identifying new NLO crystals with shorter cut-off wavelengths. High-quality organic NLO crystals must have a high NLO coefficient, UV transparency, a high laser damage threshold, and the capacity to grow readily in large dimensions [1]. Most organic compounds developed for NLO applications are derivatives of aromatic systems with donor and acceptor substituents. In their hunt for novel NLO materials with exceptional mechanical characteristics, several researchers have concentrated on tiny organic compounds with large dipole moments and chiral structure.

These molecules are typically connected via a hydrogen bond [2]. [3] Monaco et al (1987) performed an exhaustive search for novel compounds and crystals of LAP analogues. Further research in the field of amino-type compounds focused on the interaction of these materials with some chemical and inorganic substances. However, there has been little attention in the literature to novel adducts with other amino acids. The crystal structure of (L-CysH) Cl□H_2O is the first validated L-cysteine salt [4,5]. The structure was later constructed with greater accuracy in [6], and specific properties were subsequently examined in ([7,8]. L-Cysteinium hydrogen L-tartrate monohydrate was structurally studied as a potential nonlinear optical material [9,10].

Moreover, two kinds of L-cysteinium hydrogen oxalate were synthesized and structurally characterized [11,12]. [13] Giester et al (2023) followed up by determining the crystal structure of L-Cysteinium nitrate (LCN). The results showed that LCN crystallizes into an orthorhombic system with the space group $P2_12_12_1$. The unit cell parameters are: a = 5.5126 (5) Å, b = 7.9621 (7) Å, c = 17.2407 (16) Å, Z = 4, and R = 0.0372. Thermal study indicates that LCN is stable in air at temperatures between 107-110 ºC [13]. This chapter discusses the synthesis and characterisation of L-Cysteinium nitrate crystals using techniques such as single crystal XRD, FT-IR, optical absorption, optical transmission, thermal, mechanical, dielectric, and photoconductivity. [14] Kurtz and Perry's SHG test validated the crystal's NLO properties.

2. SYNTHESIS OF LCN

To make the LCN solution, an appropriate amount of high-quality L-cysteine (Sigma-Aldrich 97%) and nitric acid (Merck 69%) were mixed with water. The reaction is as follows:

$C_3H_7NO_2S + HNO_3 \rightarrow C_3H_8NO_2S^+ .NO_3^-$

To assure purity, the LCN salt was recrystallized multiple times.

1.1 GROWTH OF LCN

LCN salt was produced using an equimolar ratio of L-cysteine and nitric acid. The needed amount of L-cysteine was dissolved in double distilled water. Then, the predicted amount of nitric acid was added to the L-cysteine solution. At room temperature, the saturated solution was produced by recrystallizing mono-L-cysteinium nitrate (LCN). Seed crystals were generated through spontaneous nucleation. After 35 days of development, high grade crystals with dimensions of up to 19 x 8 x 3 mm^3 were extracted. Figure 1 displays a picture of an L-cysteinium nitrate (LCN) crystal that has grown. Table 1 shows the optimal development conditions for LCN crystals.

3. RESULT AND DISCUSSION

3.1 Single crystal X-ray diffraction

The structure of L-cysteinium nitrate (LCN) was solved directly and refined using the full matrix least-squares fit methodology with the SHELXL tool. Table 2 shows the XRD data for LCN single crystals. LCN is an orthorhombic structure system with the $P2_12_12_1$ space group. The lattice parameter values, a = 5.511 Å, b = 7.974 Å and c = 17.242 Å, are consistent with previously described values [13].

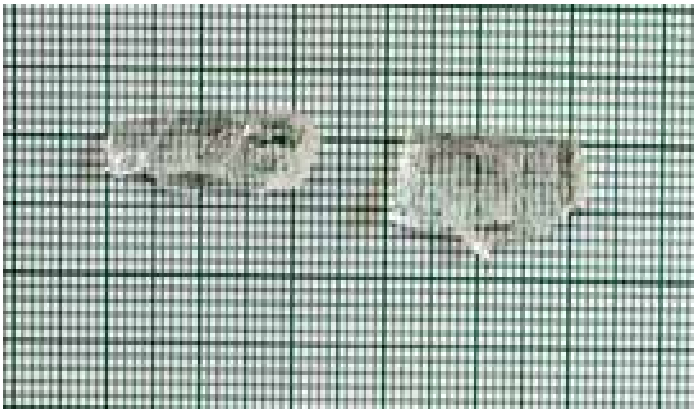


Figure 1 Photograph of as grown crystal of LCN

Table 1

Optimized growth conditions of LCN single crystal

Method of Growth	Slow solvent evaporation
Solvent used	Deionized water
Molar ratio (L-Cysteine : Nitric acid)	1:1
Temperature for growth	Room temperature (30 °C)
Period of growth	35 days
Dimension	19 x 8 x 3 mm^3

Table 2

Single crystal XRD data of LCN

Empirical formula	$C_3H_6N_2O_2S$
Crystal system	Orthorhombic
Space group	$P2_12_12_1$
a	5.511 Å
b	7.974 Å
c	17.242 Å
α	90°
β	90°
γ	90°
Volume	757.09 ($Å^3$)
Z	4

3.2 Fourier transform infrared (FTIR) spectroscopy study

Figure 2 shows the infrared spectrum of an LCN crystal. The high-frequency spectrum is predicted to reveal typical stretching vibrations for N-H, C-H, OH, and S-H bonds. The IR spectra show peaks at 2974 cm^{-1} and 2942 cm^{-1} for C-H stretching, and 3129 cm^{-1} for N-H stretching. The strength of the hydrogen bonds created determines where the OH group sits within the carboxyl group. The peak at 2624 cm^{-1} in the IR spectra corresponds to the OH group. The C=O stretching vibration at 1728 cm^{-1} indicates the existence of a carboxyl group. The NH_3^+ group has IR spectra bands at 1605 cm^{-1} and 1505 cm^{-1}, indicating asymmetric and symmetric deformation, respectively.

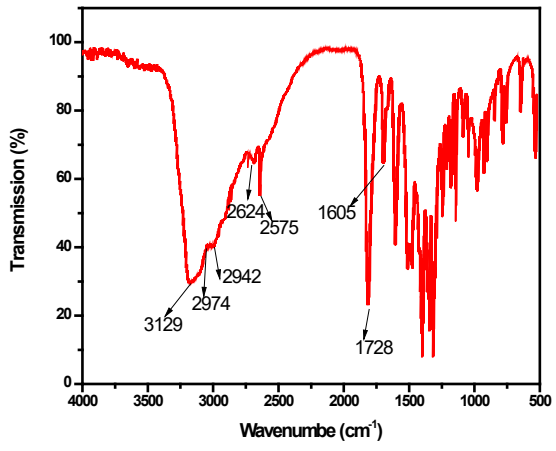


Figure 2 FT-IR spectrum of LCN crystal

3.3 Linear optical study

The UV-Vis-NIR absorbance spectra of LCN crystal was measured in the 200-1100 nm wavelength range (Figure 3). It is clear that LCN crystals have minimal optical absorption across the whole visible spectrum. The crystal has an absorbance of less than 0.2 arbitrary units. The absorption spectra of LCN shows that the lower cut-off begins at 220 nm. Figure 4 displays the optical transmission spectrum of LCN. The crystal offers good transmission over the whole visible spectrum. Transmission levels are about 80%. This transparency in the visible region is a desirable and useful feature for NLO applications. Figure 5 shows the plot of $(\alpha h\nu)^2$ versus $h\nu$, where α represents the optical absorption coefficient and $h\nu$ denotes the energy of the incident photon. The energy gap (Eg) is determined by extending the linear portion of the curve until it intersects the point where $(\alpha h\nu)^2$ equals zero. The direct band gap energy (Eg) of LCN is calculated to be 5.63 eV.

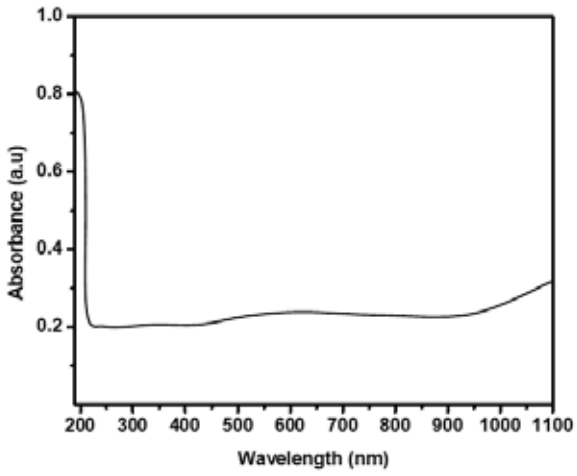


Figure 3 Optical absorption spectrum of LCN crystal

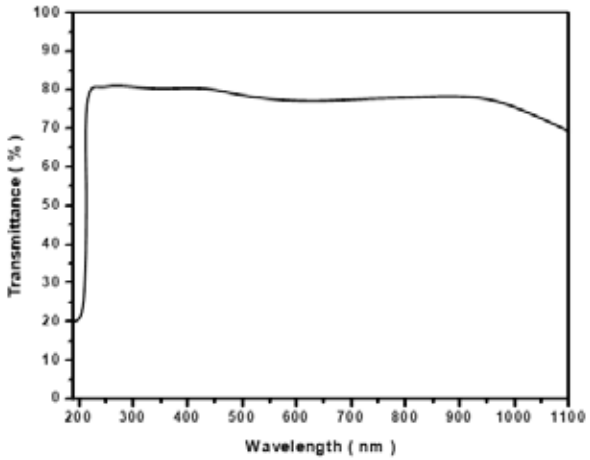


Figure 4 Optical transmission spectrum of LCN crystal

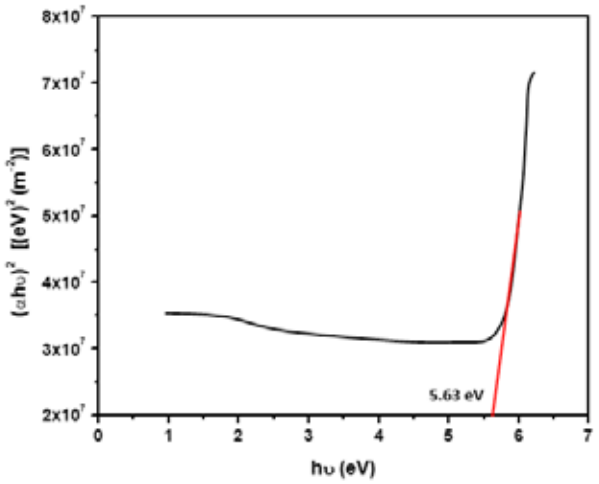


Figure 5 Tauc's plot of LCN crystal

3.4 Nonlinear optical study

The Kurtz and Perry [14] powder SHG test was performed on an LCN single crystal to determine its second harmonic generation efficiency. The crystal was subjected to a Q-switched, mode-locked Nd laser with 3.2 mJ of input pulse energy. The presence of green radiation from the crystal verified its capacity to generate second harmonic signals. LCN exhibited a second harmonic signal of 240 mV, as opposed to KDP's 160 mV. This suggests that LCN's SHG efficiency is approximately 1.5 times larger than the efficiency of KDP.

3.5 Thermal studies

The thermogravimetric and differential thermal analysis of L-cysteinium nitrate (LCN) was carried out between 28 and 400˚C in nitrogen environment, at a scanning rate of 15 ºC/min. Figure 6 depicts TGA and DTA traces. The TGA trace shows a single large weight loss beginning at roughly 126 °C. However, the DTA thermogram clearly displays an endothermic peak at 115 °C, which corresponds to the sample's melting temperature and is consistent with the value given in the literature [13]. The clarity of this exothermic peak reveals the exceptional crystallinity of the created crystal. The exothermic peaks that occur after melting indicate that the chemical is breaking down in three phases. The first stage occurs at temperatures ranging from 126-284°C. Weight loss in this region is approximately 48%, which is attributed to the loss of NH_3 and carbon dioxide molecules. The second stage of decomposition begins at 284°C, and residual degradation continues during this stage. It is clear that there is no phase change or disintegration until the melting point (115 °C). The stability of this crystal is a crucial characteristic for possible NLO applications.

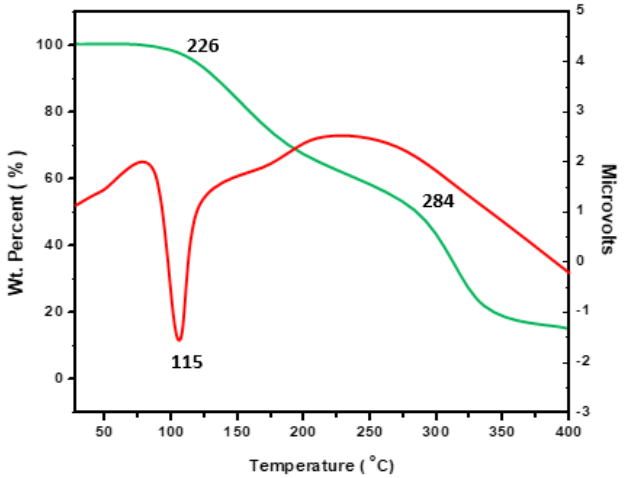


Figure 6 TGA and DTA curves of LCN

3.6 Microhardness studies

The Vickers microhardness measurement was performed on the grown crystal to determine its hardness. The microhardness test was performed using a Vickers microhardness tester equipped with a diamond pyramidal indenter. Static indentation tests were conducted on the crystal at ambient temperature. The applied force ranged from 10 to 50 gm with a constant indentation period of 10 s. Figure 7 shows how H_v varies with applied load. The graph shows that as the load increases; the microhardness number drops.

The work hardening coefficient 'n' was determined using the least squares fit approach from the plot of log P versus log d (Figure 8). The value of 'n' for LCN crystal is 3.14. For specimens that demonstrate an increase in H_v as P increases, the Meyer index n > 2, confirming typical ISE behavior [15]. Because the value of n for LCN is more than 2, the hardness of the material increases with applied load, validating Onitsch's (1956) [16] prediction.

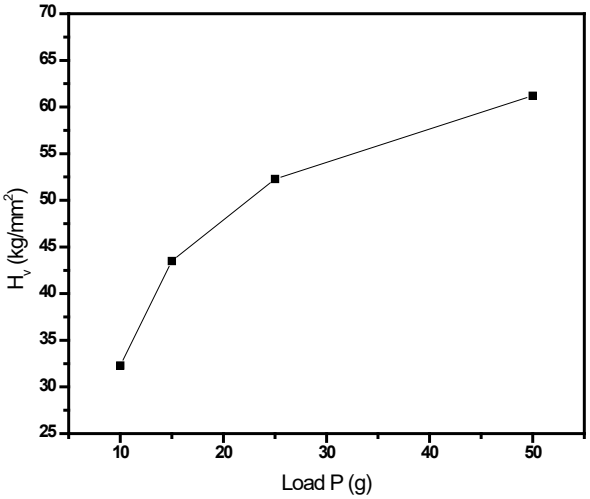


Figure 7 Plot between load P Vs Vickers Hardness for LCN

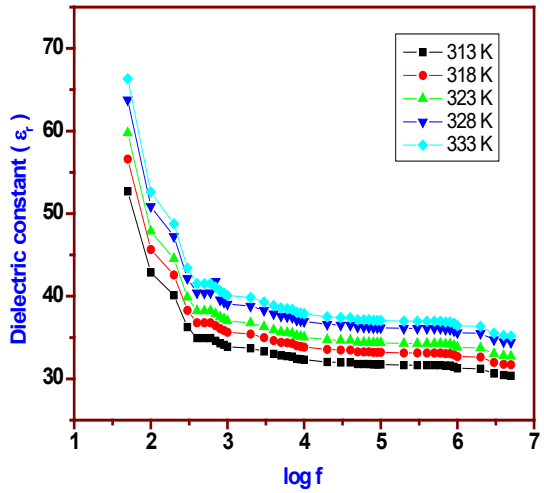


Figure 9 Variation of dielectric constant with log frequency for LCN crystal

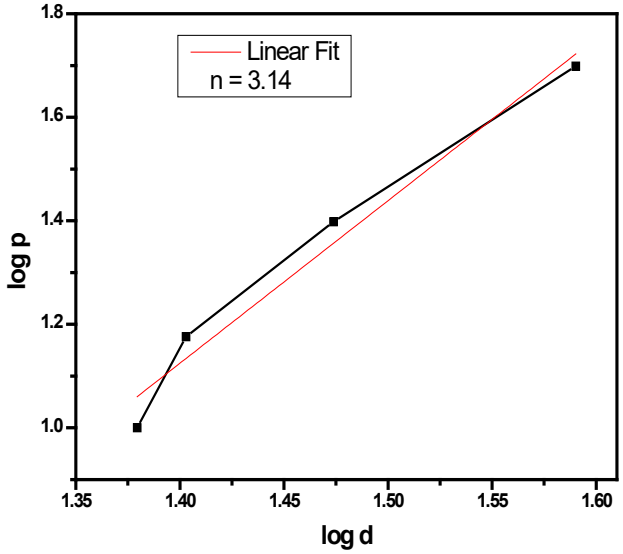


Figure 8 lot between log d Vs log P for LCN

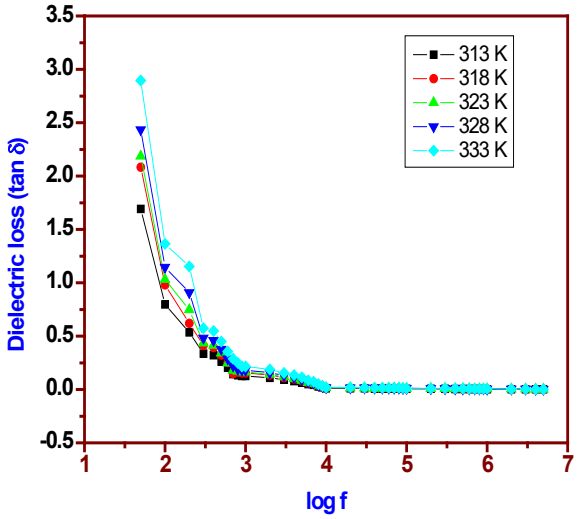


Figure 10 Variation of dielectric loss with log frequency for LCN crystal

3.7 Dielectric studies

Figures 9 and 10 demonstrate that the dielectric constant and dielectric loss of the LCN crystal vary with frequency at various temperatures (313, 318, 323, 328, and 333 K). The dielectric constant for L-cysteinium nitrate (LCN) (Figure 6.9) is 350.94 at 50 Hz and drops to 115.54 at 5 MHz. The fluctuation in the value of e_r is negligible in the frequency range of 1 kHz-5 MHz. Furthermore, both the dielectric constant and dielectric loss increase with temperature (Figure 11-12). The large value of e_r at lower frequencies could be attributable to space charge polarization.

Figure 3.10 shows that the crystal has a very low dielectric loss in the high frequency range, indicating that the crystal contains less flaws.

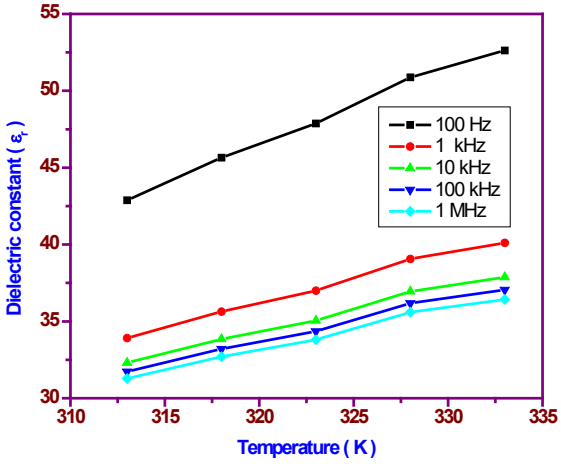


Figure 11 Variation of dielectric constant with different temperature for LCN crystal

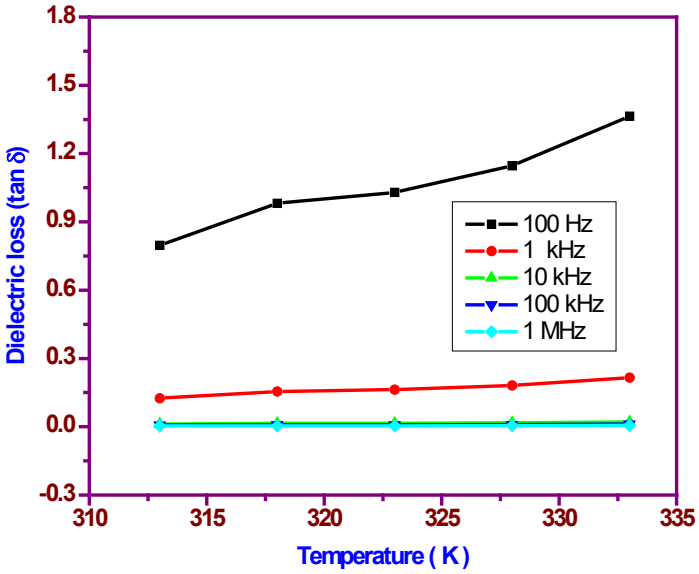
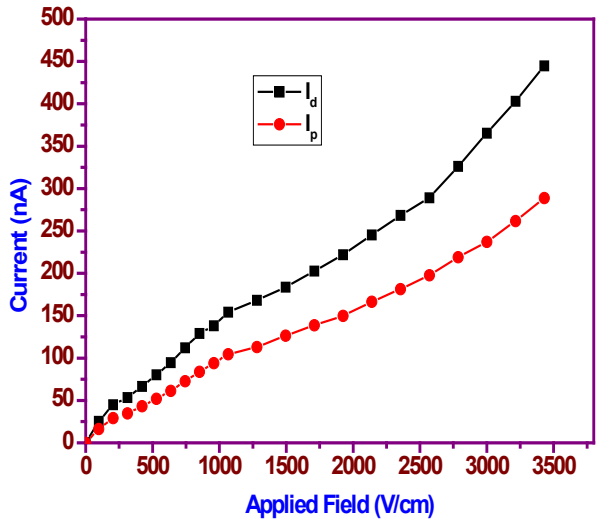


Figure 12 Variation of dielectric loss with different temperature for LCN crystal

3.8 Photoconductivity study

Photoconductivity was measured using a Keithley 485 picoammeter. The dark current was measured without exposing the sample to any radiation. Figure 13 depicts the fluctuation of dark current (I_d) and photocurrent (I_p) with applied field. The figures demonstrate that the values of the sample I_d and I_p increase linearly with the applied field. The plot shows that the dark current is always higher than the photo current, supporting the negative photoconductivity. This effect can be linked to photon absorption, which generates mobile charge carriers [17].

Figure 13 Field dependent conductivity of LCN crystal



4. CONCLUSION

Slow solvent evaporation is an efficient technique for growing LCN single crystals. X-ray diffraction studies suggest that LCN crystals are orthorhombic and belong to the $P2_12_12_1$ space group. The FT-IR spectra indicate a significant wavenumber of 1728 cm^{-1} C=O stretching vibration which is existence of a carboxyl group. The UV-Vis-NIR spectrum demonstrates that LCN has a wider transmission window and a low cut-off wavelength of 220 nm. The microhardness measurements show that the H_v value of the LCN sample rises with increasing stress, indicating that it is a soft material. Thermal investigations show that LCN remains thermally stable up to 115 °C. The reduced dielectric loss combined with high efficiency indicated that the sample has good optical quality with fewer flaws. The photoconductivity investigations demonstrate the sample's negative photoconductivity.

References

1. Shen, J., Zheng, J., Che, Y., & Xi, B. (2003). Growth and properties of organic nonlinear optical crystals: l-tartaric acid–nicotinamide and d-tartaric acid–nicotinamide. Journal of crystal growth, 257(1-2), 136-140.
2. Hameed, A. H., & Lan, C. W. (2004). Nucleation, growth and characterization of L-tartaric acid—nicotinamide NLO crystals. Journal of crystal growth, 270(3-4), 475-480.
3. Monaco, S. B., Davis, L. E., Velsko, S. P., Wang, F. T., Eimerl, D., & Zalkin, A. (1987). Synthesis and characterization of chemical analogs of L-arginine phosphate. Journal of Crystal Growth, 85(1-2), 252-255.
4. Ayyar, R. R., & Srinivasan, R. (1965). Crystal structure of l (+) cysteine hydrochloride monohydrate. Current Science, 34(15), 449-450.
5. AYYAR, R. R. (1968). Tests of the new syntheses for the solution of a structure part of which is known. Zeitschrift für Kristallographie-Crystalline Materials, 126(1-6), 282-298.
6. Chapman, R. P., & Bryce, D. L. (2007). A high-field solid-state 35/37 Cl NMR and quantum chemical investigation of the chlorine quadrupolar and chemical shift tensors in amino acid hydrochlorides. Physical Chemistry Chemical Physics, 9(47), 6219-6230.
7. Bhagavannarayana G., S. Kumar, M. Shakir, S. K. Kushawaha, K. K. Maurya, R. Malhotra, and K. R. Rao. Unidirectional growth of L-cysteine hydrochloride monohydrate: first time observation as nonlinear optical material and its characterization. J. Appl. Crystallogr., 2010, 43(4), 710-715.
8. Dourado, A. H., Silva, R. A., Torresi, R. M., Sumodjo, P. T., Arenz, M., & Cordoba de Torresi, S. I. (2018). Kinetics, Assembling, and Conformation Control of L-Cysteine Adsorption on Pt Investigated by in situ FTIR Spectroscopy and QCM-D. ChemPhysChem, 19(18), 2340-2348.
9. Shan, Y. & Huang, S. D. (1999). Z. Kristallogr. New Cryst. Struct. 214, 41–42. Sheldrick, G. M. (2008). Acta Cryst.

A64, 112–122.

10. Dhas, S. M. B., & Natarajan, S. (2008). Growth and characterization of two new NLO materials from the amino acid family: l-Histidine nitrate and l-Cysteine tartrate monohydrate. Optics Communications, 281(3), 457-462.

11. Minkov, V. S., & Boldyreva, E. V. (2008). L-Cysteinium semioxalate. Crystal Structure Communications, 64(6), 0344-0348.

12. Minkov, V. S., & Boldyreva, E. V. (2011). L-Cyste inium semioxalate: a new monoclinic polymorph or a hydrate?. Crystal Structure Communications, 67(4), 0139-0142.

13. Giester, G., Ghazaryan, V. V., Minkov, V. S., Boldyreva, E. V., & Petrosyan, A. M. (2023). L-Cysteine Nitrates. Journal of Structural Chemistry, 64(5), 917-931.

14. Kurtz, S. K., & Perry, T. T. (1968). A powder technique for the evaluation of nonlinear optical materials. Journal of applied physics, 39(8), 3798-3813.

15. Sangwal, K. (2000). On the reverse indentation size effect and microhardness measurement of solids. Materials Chemistry and Physics, 63(2), 145-152.

16. Onitsch, E.M., 1956. The present status of testing the hardness of materials. Mikroskopic. 95, 12–14

17. Joshi V.N., Photoconductivity, Marcel Dekker, New York, 1990.